AIP | Applied Physics Letters

Strain-mediated converse magnetoelectric coupling strength manipulation by a thin titanium layer

Wei-Gang Yang, Nicola A. Morley, Joanne Sharp, Ye Tian, and W. Mark Rainforth

Citation: Applied Physics Letters **108**, 012901 (2016); doi: 10.1063/1.4939111
View online: http://dx.doi.org/10.1063/1.4939111
View Table of Contents: http://scitation.aip.org/content/aip/journal/apl/108/1?ver=pdfcov
Published by the AIP Publishing

Articles you may be interested in

Direct and converse magneto-electric coupling in ferromagnetic shape memory alloys based thin film multiferroic heterostructures
Appl. Phys. Lett. **107**, 262901 (2015); 10.1063/1.4938753

Giant self-biased converse magnetoelectric effect in multiferroic heterostructure with single-phase magnetostrictive materials
Appl. Phys. Lett. **105**, 172408 (2014); 10.1063/1.4900929

In-plane anisotropic converse magnetoelectric coupling effect in FeGa/polyvinylidene fluoride heterostructure films
J. Appl. Phys. **113**, 17C705 (2013); 10.1063/1.4793780

Strain-mediated electric-field control of multiferroic domain structures in ferromagnetic films
Appl. Phys. Lett. **102**, 112407 (2013); 10.1063/1.4795938

Large converse magnetoelectric coupling in FeCoV/lead zinc niobate-lead titanate heterostructure
Appl. Phys. Lett. **94**, 082504 (2009); 10.1063/1.3086879

This article is copyrighted as indicated in the article. Reuse of AIP content is subject to the terms at: http://scitation.aip.org/termsconditions. Downloaded to IP: 143.167.213.147 On: Wed, 06 Jan 2016 09:26:18

Strain-mediated converse magnetoelectric coupling strength manipulation by a thin titanium layer

Wei-Gang Yang,[1] Nicola A. Morley,[1] Joanne Sharp,[1] Ye Tian,[2] and W. Mark Rainforth[1,a)]
[1]*Department of Materials Science and Engineering, University of Sheffield, Sheffield S1 3JD, United Kingdom*
[2]*School of Engineering and Materials Science, Queen Mary University of London, London E1 4NS, United Kingdom*

(Received 2 November 2015; accepted 13 December 2015; published online 5 January 2016)

The manipulation of the strain-mediated magnetoelectric (ME) coupling strength is investigated by inserting a thin Ti layer (0–10 nm) between a 50 nm $Co_{50}Fe_{50}$ layer and a (011) oriented lead magnesium niobate-lead titanate (PMN-PT) substrate. A record high remanence ratio (M_r/M_s) tunability of 100% has been demonstrated in the 50 nm CoFe/8 nm Ti/PMN-PT heterostructure, when a total in-plane piezoelectric strain of −1821 ppm was applied at an electric field (E-field) of 16 kV/cm. The ME coupling strength is gradually optimized as the Ti layer thickness increases. Magnetic energy calculation showed that with increasing Ti layer thickness the uniaxial magnetic anisotropy energy (E_{uni}) was reduced from 43 ± 1 kJ/m^3 to 29.8 ± 1 kJ/m^3. The reduction of E_{uni} makes the strain effect dominant in the total magnetic energy, thus gives an obvious enhanced ME coupling strength. © *2016 AIP Publishing LLC*. [http://dx.doi.org/10.1063/1.4939111]

Magnetoelectric (ME) coupling[1] in multiferroic[2] (MF) composites has drawn intensive interest due to their important potential applications such as low-power spintronic devices.[3] In recent years, many papers[4–9] have reported the obvious strain-mediated converse ME coupling in a wide range of the MF layered heterostructure. Both magnetization and magnetic anisotropy of the magnetic film can be manipulated by an external electric field (E-field) induced piezoelectric strain, which provides great opportunities for E-field controlling magnetic devices. However, the manipulation of ME coupling strength is much less investigated. Kim *et al.*[10] studied the manipulation of ME coupling strength by varying the composition and thickness of the Co_xPd_{1-x} film. A large ME coupling strength was found for 10 nm $Co_{0.25}Pd_{0.75}$ film due to a high magnetostriction. The effect of the underlayer on magnetic thin films has been widely studied[11–13] in the past few decades. The reason can be attributed to the thin underlayer leading a change of the texture and the stress in the magnetic thin films. Jung and Doyle[13] found that a thin Cu underlayer changed the preferred orientation from (200) to (110) in the CoFe film and thus improved the magnetic softness. In our work, the effect of the introduction of a thin Ti layer on the converse ME coupling strength was carried out. A record high remanence ratio (M_r/M_s) tunability of 100% has been demonstrated in the 50 nm CoFe/8 nm Ti/PMN-PT heterostructure. In addition, our previous results[14,15] have demonstrated a promising ME coupling effect in the $Co_{50}Fe_{50}$ (CoFe)/(011) PMN-PT heterostructure.

50 nm thick CoFe/x nm Ti films (x = 0, 2, 4, 6, 8, 10) were RF sputtered on the (011) oriented PMN-30%PT substrate with mean surface roughness 1.31 ± 0.08 nm at room temperature. The polished substrate[15] was cleaned prior to use with n-Butyl acetate, acetone, and IPA. The sputtering power, working pressure, and base pressure were 75 W, 5.0 ± 0.1 mTorr, and $1.2 \pm 0.2 \times 10^{-3}$ mTorr, respectively. An *in-situ* magnetic field (H-field) of 65.3 kA/m was applied along the [100] crystallographic direction of the PMN-PT substrate during the growth of the CoFe film for obtaining a maximum normalized remanence (M_r/M_s) ratio (∼1) and thus maximum variation in M_r/M_s. The (011)PMN-PT (10 cm [01–1] × 5 cm [100] × 0.5 cm [011]) had anisotropic strains with in-plane piezoelectric coefficients of $d_{31} = -1200$ to -1800 pC/N reported by H.C. Materials Corporation. The piezoelectric constant d_{33} was measured to be 400 ± 10 pC/N for all these substrates on a d_{33} testing meter. The difference between all PMN-PT substrates used in this work was ∼2.5%. The polarization (P) and out of plane piezoelectric strain (ε_z) of the (011) PMN-PT substrate as a function of the E-field were measured using triangular voltage waveforms by a ferroelectric hysteresis measurement tester (National Physics Laboratories, UK).[16] The piezoelectric strain was converted to a voltage signal by a pair of NXB2-AL nanosensors and sent to a digital voltmeter for acquiring data.[17] When the overall volume of the substrate is kept constant, the in-plane piezoelectric strain (ε_{x+y}) is $-\varepsilon_z$. Magneto-Optical Kerr Effect (MOKE) measurements were used to investigate the magnetic properties when a large range dc E-fields (0–17 kV/cm) were applied to the MF heterostructures. The MOKE H-field was applied along the [100] or [01-1] direction of the PMN-PT, while the E-field was applied along [011] direction of the PMN-PT. More detailed measurement methods are found in Refs. 14 and 15. The CoFe film and the bottom Au on the PMN-PT surface were used as the electrodes. To test the CoFe electrode, the electric capacity was measured to be about 3000 pF using an impedance analyzer, which is comparable with a sample with two Au electrodes. The effective saturation magnetostriction constants (λ_{eff}) were measured using a technique[15,18] based on the Villari effect. To investigate the microstructure of the heterostructure, X-ray diffraction (XRD) measurements were made on the samples using a Siemens D5000 X-ray diffractometer with CuK_α radiation.

a)Electronic mail: m.rainforth@sheffield.ac.uk

 © 2016 AIP Publishing LLC

This article is copyrighted as indicated in the article. Reuse of AIP content is subject to the terms at: http://scitation.aip.org/termsconditions. Downloaded to IP: 143.167.213.147 On: Wed, 06 Jan 2016 09:26:18

Cross-sectional transmission electron microscopy (TEM) specimens were prepared by Focused Ion Beam (FIB) in FEI Quanta 200 3D. The fabricated TEM specimens were observed on a JEOL R005 operating at 300 kV.

Figure 1(a) shows the XRD patterns of the 50 nm CoFe/x Ti/PMN-PT heterostructures at a scan speed of 0.23 °/min and 65 nm CoFe/PMN-PT heterostructures at a scan speed of 0.5 °/min. It shows strong (011) and (022) diffraction peaks for the PMN-PT substrate. The vertical lines indicate the 2θ position of the standard diffraction peaks (110) and (002) (cited from PDF#04-003-5514) for the CoFe film. The weak (110) diffraction peak of CoFe film at $2\theta = 44.9°$ is only seen on a smaller intensity scale (inset), while the (002) diffraction peak at $2\theta = 65.3°$ overlaps with the strong PMN-PT (022) peak at $2\theta = 65.5°$ and thus it is hard to be observed. The (110) peak of CoFe is clearly observed for 50 nm CoFe without Ti; however, the peak disappears when the Ti layer was added, with all data being taken with the same scan conditions. This suggests that the Ti layer promotes random orientation of the CoFe grains, which is helpful to reduce the magnetocrystalline anisotropy energy contribution to total magnetic energy and thus to make the magnetoelastic energy dominant. In Fig. 1(c), the High Angle Annular Dark Field (HAADF) image shows a columnar growth structure of CoFe film and an average columnar grain size of 3.6 ± 0.5 nm in the CoFe/8 nm Ti/PMN-PT heterostructure, which is almost same as that of 3.3 ± 0.5 nm in the CoFe/PMN-PT heterostructure.[15] Selected area electron diffraction (SAED) pattern shows the polycrystalline structure of CoFe film. However, the crystalline plane of (110) in CoFe film for the CoFe/8 nm Ti/PMN-PT heterostructure shows weaker diffraction than that for the CoFe/PMN-PT heterostructure,[15] which is consistent with XRD results of CoFe film.

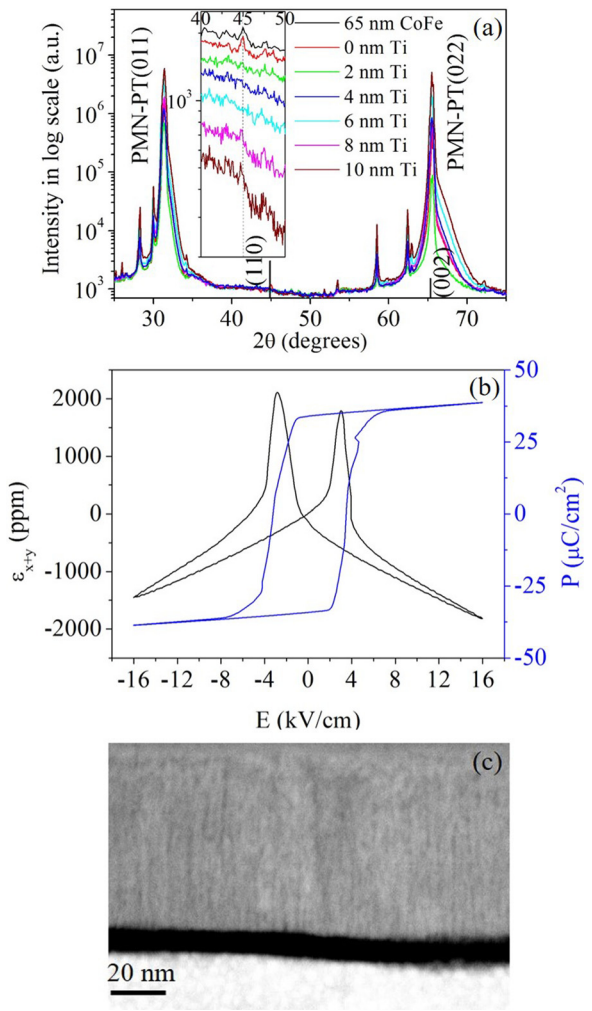

FIG. 1. (a) XRD spectra of 50 nm CoFe/x nm Ti/PMN-PT and 65 nm CoFe/PMN-PT heterostructures. The inset shows an enlarged part around the (110) diffraction peak of the CoFe film. (b) Ferroelectric hysteresis loop and in-plane piezoelectric strain loop of (011) oriented PMN-PT. (c) The HAADF image of the CoFe/8 nm Ti/PMN-PT heterostructure.

Figure 1(b) shows the P and ε of (011) PMN-PT substrate as a function of the E-field. The ferroelectric and piezoelectric properties were studied at an alternating E-field with a maximum amplitude of 16 kV/cm and a frequency of 0.5 Hz. The maximum in-plane compressive strain ε_{x+y} is ~1821 ppm at 16 kV/cm. The ferroelectric coercive field is ~3.5 kV/cm and slightly higher compared with ~2 kV/cm reported previously,[19] which results in the larger operational E-field up to around 16 kV/cm compared with the reported[20,21] 10 kV/cm for PMN-PT single crystal.

Figures 2(a) and 2(b) show the strong E-field dependence of the hysteresis loops measured along [01-1] and [100] in 50 nm CoFe/8 nm Ti/PMN-PT heterostructure, respectively. For the other samples, a strong E-field dependence of the hysteresis loops was also observed at the higher applied E-field, but is not shown in this paper. As we can see, the magnetization process along [01-1] becomes easy, while that along [100] becomes hard with the applied E-field. The results can be qualitatively analysed by the strain induced domain wall motion. The magnetoelastic energy can be described as[22]

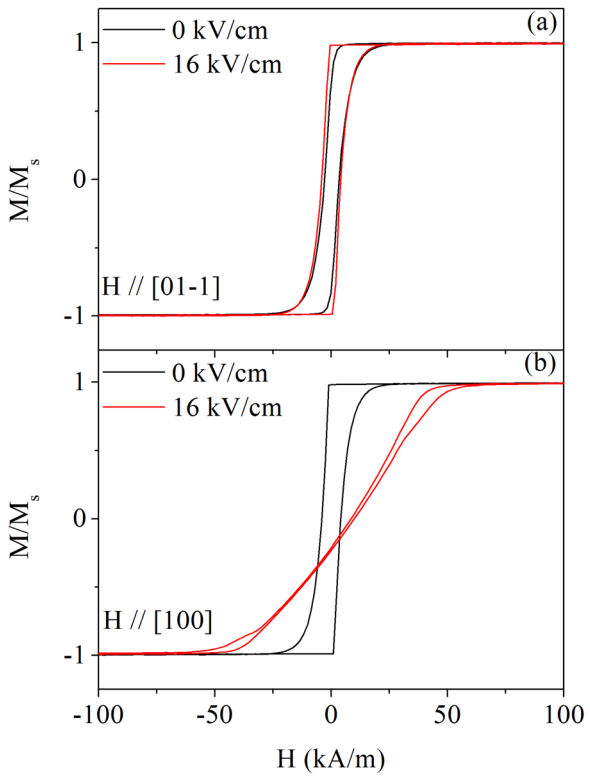

FIG. 2. Electric dependence of magnetic hysteresis loops measured along [01-1] (a) and [100] (b) in 50 nm CoFe/8 nm Ti/PMN-PT heterostructure.

This article is copyrighted as indicated in the article. Reuse of AIP content is subject to the terms at: http://scitation.aip.org/termsconditions. Downloaded to IP: 143.167.213.147 On: Wed, 06 Jan 2016 09:26:18

$$E_{stress} = (-3/2)\lambda\sigma\cos^2\theta, \quad (1)$$

where λ and σ are magnetostriction constant and stress, while θ is the angle between the saturation magnetisation (M_s) and σ. For minimizing the E_{stress} in the system, the external E-field induces tensile strain (i.e., $\sigma > 0$) along [01–1], causing more magnetic moments to align along this tensile stress direction due to the positive λ. When the H-field is applied along [01-1], a lower H-field will be required to saturate the sample due to the relatively easy 180° wall motion.[22] In contrast, the compressive stress ($\sigma < 0$) along [100] causes more magnetic moments to align perpendicular to [100]. Thus, when the H-field is applied along [100], a higher H-field is required to rotate the magnetic moments 90° into the [100] direction. Here, the E-field induced stress field plays the same role to move the domain wall in the magnetization process as that of the H-field. However, the domain rotation has to be completed by the H-field. Furthermore, the stress field induced domain motion can make the domain rotation easier or harder by the H-field.

Figures 3(a) and 3(b) show the detailed variation in the M_r/M_s, taken from the magnetic hysteresis loops measured along [01-1] and [100] at each applied E-field in these heterostructures. When the E-field is increased, the M_r/M_s is increased along the [01-1] direction and reduced along the [100] direction in all the samples. As the E-field is increased further, the M_r/M_s along [01-1] is almost constant close to 1, while the M_r/M_s along [100] is decreased as the E-field is increased. At the E-field of 17 kV/cm, the maximum M_r/M_s change along [100] is 72% for the sample without Ti layer, while a larger M_r/M_s change of 100% is reached at the E-field of 16 kV/cm for the sample with 8 nm Ti layer. This suggests that the addition of a Ti layer significantly improves the converse ME coupling strength.

The total magnetic energy (E_{total}) of the samples can be described as[21]

$$E_{total} = E_{zeeman} + E_{shape} + E_{stress} + E_{charge} + E_{uni}, \quad (2)$$

where E_{zeeman}, E_{shape}, E_{stress}, E_{charge}, and E_{uni} are the Zeeman energy, demagnetizing energy, magnetoelastic energy, charging induced surface anisotropy energy, and uniaxial magnetic anisotropy energy, respectively. In the present work, only the last three energy terms are changed. First, when the conductive Ti layer is introduced into the interface between the CoFe and the PMN-PT substrate, the charge accumulation is hindered on the interface due to the metallic short charge screening length.[21] Therefore, E_{charge} is reduced in the sample with the Ti layer. Next, the E_{uni} can be calculated as:[23] $E_{uni} = (1/2)H_kM_s$, where the anisotropy field H_k is taken from the measured hysteresis loop at the $M/M_s = 1$ and shown in Fig. 3(d) and M_s is 1900 emu/cm^3 taken from Ref. 24. As shown in Fig. 3(d), when the Ti thickness increases, the E_{uni} is gradually reduced. For the sample without a Ti layer, the E_{uni} is 43 ± 1 kJ/m^3, while the E_{uni} is 29.8 ± 1 kJ/m^3 in the sample with 8 nm Ti. Therefore, the E_{uni} is reduced by 13.2 kJ/m^3 in the 8 nm Ti sample. The anisotropy change also can be clearly observed in the inset of Fig. 3(a), which shows the M_r/M_s measured along a series of angles for the 0 nm and 8 nm Ti samples.

The other contribution to the ME coupling strength change by the Ti layer is the increasing E_{stress} due to the varying λ. In a (110) textured film, the λ is given by $\lambda_{(110)} = (1/5)\lambda_{100} + (4/5)\lambda_{111} = 54$ ppm, while in a randomly orientated polycrystalline film, λ is given by $\lambda_{isotropic} = (2/5)\lambda_{100} + (3/5)\lambda_{111} = 78$ ppm, where λ_{100} and λ_{111} are magnetostriction constant along the [100] and [111] of a single crystal, 150 ppm and 30 ppm, respectively.[25] As discussed in the XRD results (Fig. 1(a)), the (110) texture exists in the sample without Ti layer, while the texture disappears in the sample with a Ti layer. Therefore, the λ can be altered due to the texture change in the CoFe film. The λ is estimated by measuring the same grown films on the Si substrate. As shown in Fig. 3(c), the effective saturation magnetostriction constant λ_{eff} increases from 37 ± 2 ppm to 48 ± 2 ppm, as the Ti layer thickness increases from 0 nm to 4 nm.

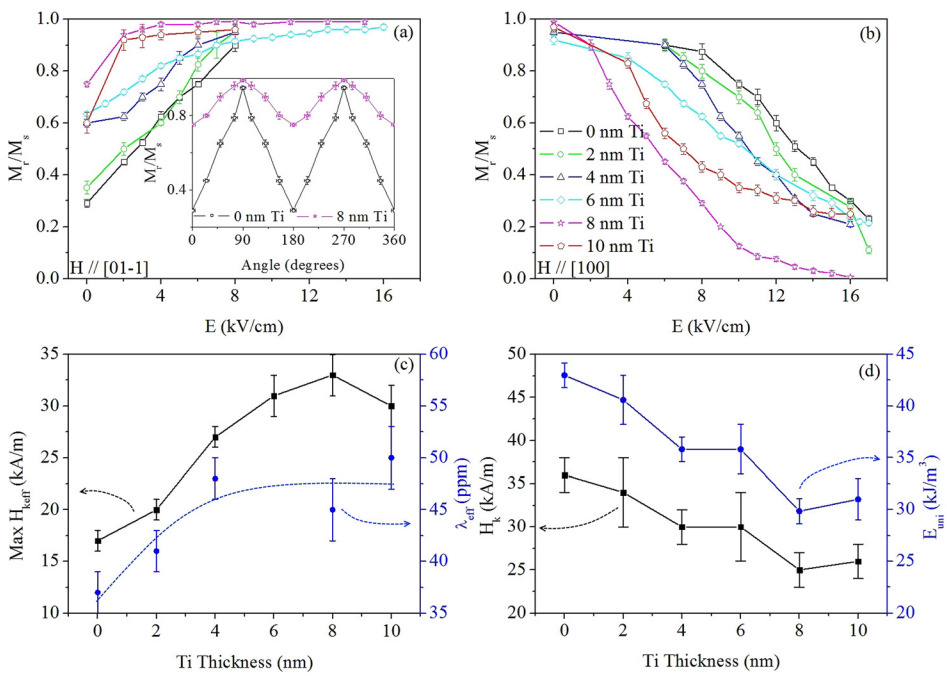

FIG. 3. (a) and (b) The normalized remanence (M_r/M_s) as a function of applied E-field in 50 nm CoFe/x nm Ti/PMN-PT heterostructure along [01-1] and [100], respectively. The inset shows the angular dependence of M_r/M_s. The 0° corresponds to the [01-1] direction of PMN-PT substrate. (c) The E-field induced maximum effective anisotropy field H_{keff} and the effective saturation magnetostriction constant λ_{eff}. (d) The anisotropy field H_k without the applied E-field and the calculated E_{uni} for the different Ti thickness.

This article is copyrighted as indicated in the article. Reuse of AIP content is subject to the terms at: http://scitation.aip.org/termsconditions. Downloaded to IP: 143.167.213.147 On: Wed, 06 Jan 2016 09:26:18

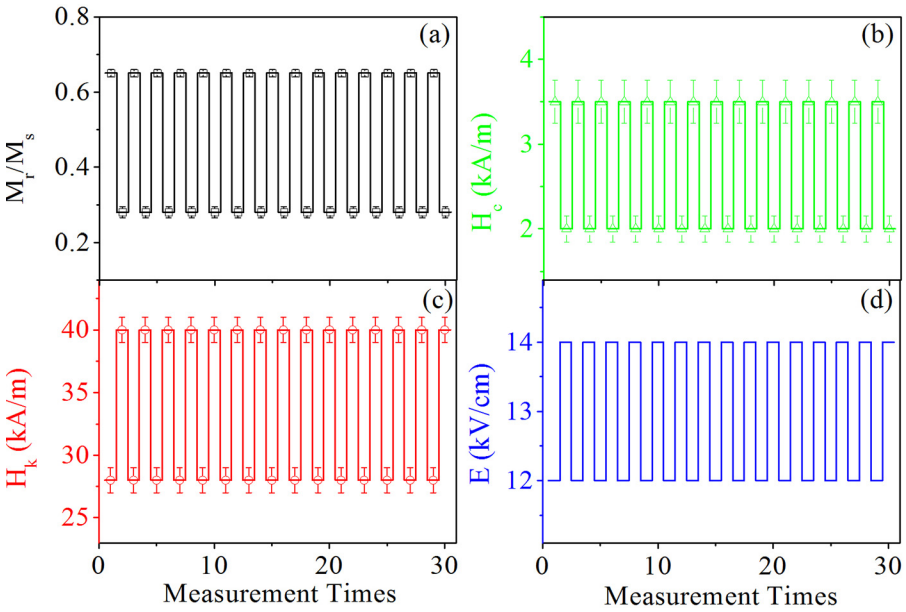

FIG. 4. E-field induced reproducible and quick magnetic properties change in the CoFe thin film.

However, when the Ti thickness increases from 4 to 10 nm, the λ_{eff} is almost constant. Based on the measured λ, the E_{stress} can be deduced to be increase as $E_{stress} = 3/2\lambda\varepsilon Y$,[23] where Y is Young's modulus of CoFe. Therefore, the energy reduction of E_{charge} and E_{uni} and meanwhile the increase of E_{stress} make the E_{stress} contribution to the E_{total} dominant, thus produces the stronger converse ME coupling.

To investigate the repeatability of the ME coupling, Figs. 4(a)–4(d) show the magnetic properties change induced by E-field, when the E-field is applied at 12 kV/cm, then at 14 kV/cm and repeated for 30 measurements. Each magnetic hysteresis loop measurement takes about 30 s in the high H-field MOKE. The heterostructure shows a stable magnetization switching between these high E-fields. Previously, the most dynamic E-field impulse induced magnetization switching[6,21] was carried out at fields lower than 8 kV/cm for PMN-PT substrates due to the poor FE stability at the high E-field range. The results in this work suggest potential applications in high voltage handling capability and high output power devices.

In summary, the effect of the introduction of a Ti layer on the converse ME coupling strength was investigated. Both the interface structure and the film structure were altered by the Ti layer. The addition of the Ti layer reduced the contribution of the original magnetic anisotropy energy to the total magnetic energy, which resulted in the enhanced converse ME coupling strength. In addition, these heterostructures also show good high-voltage stability suggesting potential applications in high voltage handling capability and high output power devices.

This work was financially supported by a University of Sheffield Prize Scholarship.

[1]C. Israel, N. D. Mathur, and J. F. Scott, Nat. Mater. **7**, 93 (2008).
[2]W. Eerenstein, N. D. Mathur, and J. F. Scott, Nature **442**, 759 (2006).
[3]E. Y. Tsymbal, Nat. Mater. **11**, 12 (2012).
[4]Y. Zhang, Z. Wang, Y. Wang, C. Luo, J. Li, and D. Viehland, J. Appl. Phys. **115**, 084101 (2014).
[5]M. Liu, S. D. Li, O. Obi, J. Lou, S. Rand, and N. X. Sun, Appl. Phys. Lett. **98**, 222509 (2011).
[6]M. Liu, Z. Y. Zhou, T. X. Nan, B. M. Howe, G. J. Brown, and N. X. Sun, Adv. Mater. **25**, 1435 (2013).
[7]M. Liu, O. Obi, J. Lou, Y. J. Chen, Z. H. Cai, S. Stoute, M. Espanol, M. Lew, X. Situ, K. S. Ziemer, V. G. Harris, and N. X. Sun, Adv. Funct. Mater. **19**, 1826 (2009).
[8]J. H. Park, Y. K. Jeong, S. Ryu, J. Y. Son, and H. M. Jang, Appl. Phys. Lett. **96**, 192504 (2010).
[9]T. Wu, A. Bur, P. Zhao, K. P. Mohanchandra, K. Wong, K. L. Wang, C. S. Lynch, and G. P. Carman, Appl. Phys. Lett. **98**, 012504 (2011).
[10]J. H. Kim, K. S. Ryu, J. W. Jeong, and S. C. Shin, Appl. Phys. Lett. **97**, 252508 (2010).
[11]S. X. Wang, N. X. Sun, M. Yamaguchi, and S. Yabukami, Nature **407**, 150 (2000).
[12]N. X. Sun and S. X. Wang, J. Appl. Phys. **92**, 1477 (2002).
[13]H. S. Jung and W. D. Doyle, IEEE Trans. Magn. **38**, 2015 (2002).
[14]W.-G. Yang, N. A. Morley, and W. M. Rainforth, J. Appl. Phys. **118**, 034102 (2015).
[15]W.-G. Yang, N. A. Morley, J. Sharp, and W. M. Rainforth, J. Phys. D: Appl. Phys. **48**, 305005 (2015).
[16]H. Yan, F. Inam, G. Viola, H. Ning, H. Zhang, Q. Jiang, T. Zeng, Z. Gao, and M. J. Reece, J. Adv. Dielectr. **01**, 107 (2011).
[17]G. Viola, T. Saunders, X. Wei, K. B. Chong, H. Luo, M. J. Reece, and H. Yan, J. Adv. Dielectr. **3**, 1350007 (2013).
[18]A. Javed, N. A. Morley, and M. R. J. Gibbs, J. Magn. Magn. Mater. **321**, 2877 (2009).
[19]T. Wu, P. Zhao, M. Bao, A. Bur, J. L. Hockel, K. Wong, K. P. Mohanchandra, C. S. Lynch, and G. P. Carman, J. Appl. Phys. **109**, 124101 (2011).
[20]T. Fitchorov, Y. Chen, B. Hu, S. M. Gillette, A. Geiler, C. Vittoria, and V. G. Harris, J. Appl. Phys. **110**, 123916 (2011).
[21]T. Nan, Z. Zhou, M. Liu, X. Yang, Y. Gao, B. A. Assaf, H. Lin, S. Velu, X. Wang, H. Luo, J. Chen, S. Akhtar, E. Hu, R. Rajiv, K. Krishnan, S. Sreedhar, D. Heiman, B. M. Howe, G. J. Brown, and N. X. Sun, Sci. Rep. **4**, 3688 (2014).
[22]B. D. Cullity and C. D. Graham, *Introduction to Magnetic Materials* (Wiley, Hoboken, 2009).
[23]C.-J. Hsu, J. L. Hockel, and G. P. Carman, Appl. Phys. Lett. **100**, 092902 (2012).
[24]T. L. Jin, L. Hao, J. W. Cao, M. F. Liu, H. G. Dang, Y. Wang, D. P. Wu, J. M. Bai, and F. L. Wei, Appl. Phys. Express **7**, 043002 (2014).
[25]R. C. Hall, J. Appl. Phys. **31**, S157 (1960).

This article is copyrighted as indicated in the article. Reuse of AIP content is subject to the terms at: http://scitation.aip.org/termsconditions. Downloaded to IP: 143.167.213.147 On: Wed, 06 Jan 2016 09:26:18